Asymmetric Mechanosensitivity in a Eukaryotic Ion Channel

Michael V. Clausen, Viwan Jarerattanachat, Elisabeth P Carpenter,

Mark S.P. Sansom and Stephen J. Tucker

[1] Clarendon Laboratory, Department of Physics, University of Oxford, Oxford, UK; [2] Department of Biochemistry, University of Oxford, Oxford, UK; [3] OXION Initiative in Ion Channels and Disease, University of Oxford, Oxford, UK; [4] Structural Genomics Consortium, University of Oxford, UK.

Correspondence to: *stephen.tucker@physics.ox.ac.uk*

Key Words: *K2P channel; KCNK10; TREK-2; Mechanosensitive; K^+ channel gating.*

ABSTRACT

Living organisms perceive and respond to a diverse range of mechanical stimuli. A variety of mechanosensitive ion channels have therefore evolved to facilitate these responses, but the molecular mechanisms underlying their exquisite sensitivity to different forces within the membrane remains unclear. TREK-2 is a mammalian two-pore domain (K2P) K^+ channel important for mechanosensation and recent studies have shown how increased membrane tension favors a more expanded conformation of the channel within the membrane. However, these channels respond to a complex range of mechanical stimuli and it is uncertain how differences in tension between the inner and outer leaflets of the membrane contribute to this process. To examine this, we have combined computational approaches with functional studies of oppositely oriented single channels within the same lipid bilayer. Our results reveal how the asymmetric structure of TREK-2 enables it to distinguish a broad profile of forces within the membrane and thereby illustrates the mechanisms that eukaryotic mechanosensitive ion channels may utilize to detect and fine-tune their response to different mechanical stimuli.

SIGNIFICANCE STATEMENT.

One important way that living organisms are able to detect and respond to their environment is via the conversion of mechanical forces into electrical signals. However, the molecular mechanisms that enable mammalian ‘mechanosensitive’ ion channels to detect a wide profile of forces within the membrane remain unclear. By studying the functional activity of individual TREK-2 K2P channels inserted in different directions into a lipid bilayer we are now able to describe how the asymmetric structure of this channel enables it to sense such a broad profile of forces. These results help us to understand how eukaryotic ion channels respond to a rich variety of sensory stimuli.

\body

Introduction

Many forms of sensory perception in higher organisms depend upon the rapid conversion of mechanical and physical stimuli into the electrochemical language of nerve and muscle cells (1). These transduction mechanisms often involve 'mechanosensitive' (MS) ion channels that are able to rapidly convert physico-mechanical stimuli into the electrical signals required for complex physiological responses e.g. touch, pain, hearing and proprioception, as well those mechanical signals that play key roles in development and cell-cell communication (2). The enormous complexity and diversity of these sensory responses suggests that a variety of molecular mechanisms are likely to be responsible. For example, whilst some channels are regulated via physical coupling to proteins of the cytoskeleton and/or cell matrix, others directly respond to changes in lipid membrane tension (3). However, the precise structural and physical mechanisms underlying these processes remain poorly understood (4-6).

Our current understanding of how membrane tension directly regulates ion channel gating is largely derived from studies of prokaryotic MS ion channels involved in the control of bacterial turgor pressure (7, 8). The open state of these MS channels has a larger cross-sectional area than the closed state within the membrane, and stretch-induced changes in the forces within the bilayer stabilize the expanded open state conformation. This is commonly referred to as the *force-from-lipid* principle of mechanosensitivity (9). Similar physical principles are thought to regulate many eukaryotic MS channels (5, 10).

Typically, the functional activity of MS ion channels is examined in pipette-based patch-clamp recordings in which negative or positive pressures are used to alter bilayer tension. These pressure changes stretch the membrane to alter the lateral pressure profile i.e. the complex profile of forces that vary with location across the bilayer (11-13). MS channels embedded within the bilayer have been shown to directly respond to these changes (14, 15). The application of either positive or negative pressure increases the overall tension within both leaflets of the bilayer, and there is now a large body of evidence demonstrating how such changes in lateral tension underlie

the activation of MS channels (2-5). However, within their cellular environment eukaryotic MS channels are able to respond to a diverse and complex range of mechanical stimuli such as changes in osmotic and mechanical pressure, strain and shear forces, acceleration, vibration and sound etc., all of which may modify membrane mechanics in a myriad of different ways. Thus for intrinsically mechanosensitive channels gated solely by membrane tension it seems unlikely that symmetrical changes in lateral membrane tension alone (i.e. equal changes in both leaflets) can fully explain the complexity of their response and the rich variety of physiological processes that MS channels are able to control. Interactions with the cytoskeleton and other proteins will undoubtedly influence their response (1), but a fundamental understanding of their intrinsic response to changes in bilayer tension is still required. A number of computational and theoretical studies of membrane tension have emphasized how stretch-induced changes in the lateral pressure profile may not be symmetrical between the two leaflets (i.e. inner and outer) of the lipid bilayer and how this may influence gating (16-20), but these studies are mostly restricted to prokaryotic MS channels. More tractable and better defined experimental systems for the study of eukaryotic MS channels are therefore needed.

TREK-2 is a eukaryotic mechanosensitive ion channel that belongs to the Two-Pore Domain (K2P) family of K^+-selective channels and is important for mechanical and thermal nociception in many sensory neurons (21, 22). Other members of this subgroup of mechanosensitive K2P channels include TREK-1 and TRAAK. All three channels have now been shown to respond directly to changes in membrane tension (23, 24), and their mechanosensitivity is thought to be important for many diverse physiological processes, e.g. electromechanical feedback in the heart, cell volume regulation and perception of shear flow stress in epithelial tissues, pressure induced vasorelaxation in endothelia, and even cell migration (25-28). Crystal structures are also now available for these three channels in multiple conformations (29-32). Therefore, they represent an excellent opportunity to investigate the molecular mechanisms underlying mechanosensitivity in eukaryotic ion channels.

We have recently shown how increased (symmetrical) lateral tension within the lipid bilayer induces a structural change in TREK-2 from the 'Down' state of the channel to the more expanded 'Up' state conformation (31, 33, 34). However, unlike the non-selective prokaryotic MS channels where stretch-induced expansion dilates the central pore, K2P channels remain highly K^+-selective (35). Therefore, it is perhaps not surprising that stretch-induced expansion in TREK-2 occurs primarily via movement in the lower half of the protein, i.e. away from the filter and within the cytoplasmic inner leaflet alone (**Figure 1**). Thermodynamic descriptions of mechanogating refer to asymmetric structural changes like this as 'shape sensitivity'. In addition to changes in overall cross-sectional area, this represents one of the main types of conformational change thought to underlie the 'mechanosensitivity' of integral membrane proteins (13, 36, 37).

One prediction of this shape sensitivity for TREK-2 is that it should also allow the channel to detect an increase in tension within an individual leaflet of the bilayer. Differences in tension between the two leaflets not only result in an asymmetry of the lateral pressure profile, but also generate additional forces across the membrane known as 'membrane torque' (36, 38). Typically, such asymmetric changes are elicited either by alterations in membrane curvature, or via insertion of non-cylindrical lipids into individual leaflets (36, 39). There is extensive evidence for the effects of non-cylindrical lipids on TREK channel function (40, 41), as well as for asymmetric effects of the mechanosensitive toxin, GsMTx4 (42). However, conflicting reports about the response of TREK channels to negative *vs*. positive pressure (23, 24, 43) means that the contribution of membrane curvature and shape-sensitivity to K2P channel mechanosensitivity remains unclear.

In this study, we have used a combination of functional and computational approaches to investigate how the different structural states of TREK-2 define its response to membrane tension. Importantly, our results provide clear evidence of an asymmetric response to changes in bilayer tension that allows TREK-2 to detect a broad profile of forces within the membrane. Overall, this highlights the complex role the bilayer environment plays in the gating of a eukaryotic mechanosensitive ion channel.

Results

Structural changes in response to asymmetric membrane tension. Increasing lateral membrane tension within the bilayer is associated with an increase in the area per lipid and free volume within the membrane (14, 44). In our previous study, we used a well-established MD simulation approach to simulate these effects of membrane stretch (34). This method of symmetrically stretching the membrane increased the area per lipid in both the inner and outer leaflets of the bilayer at the same time and elicited a structural transition in TREK-2 from the 'Down' to the 'Up' state (**Figure 1B**). However, the resultant change in cross-sectional area of the channel is almost exclusively confined to the inner leaflet and thus highly asymmetric (**Figure 1C and 1D**). We therefore examined whether an increase in tension confined to the inner leaflet alone is sufficient to drive this structural transition. Previous studies of prokaryotic MS channel activation have used the addition of molecules to a single leaflet to generate differences in monolayer stresses (45). However, in the approach used here, the area of the simulation box in the plane of the bilayer was kept constant, and lipids were selectively removed from a single leaflet (either inner or outer). This generated an increase in area per lipid in a single leaflet equivalent to the increase in tension used previously in our (symmetrical) stretch protocols (34) (**Figure 2A,** see methods for details).

This 'asymmetric stretch' protocol did not cause any major alteration in the shape of the bilayer (**Figure 2A**), but it did produce an asymmetric change in the lateral pressure profile across the bilayer (**Figure 2B**). In particular, a large decrease in the positive pressures was produced by the lipid tails within the core of the bilayer when their number was reduced, with a concomitant increase in lateral tension at the interfacial region near the headgroups. A small compensatory increase in positive pressures was also seen in the opposite leaflet, but overall the changes are restricted to the leaflet where lipids are removed. To monitor any conformational changes in TREK-2 we compared the root-mean-square deviation (RMSD) of the Cα atoms for the TM helices (M1-M4) against the Up-state crystal structure (PDB ID: 4BW5). This measurement provides an

estimate of how closely the structure resembles the Up-state conformation. Interestingly, when tension was increased within the inner leaflet alone it induced a conformational change towards the Up-state over the course of a 200 ns simulation to produce a structure similar to that induced by symmetrical tension (**Figure 2B and 2C**). By contrast, no movement towards the up state was seen when tension was altered in the outer leaflet alone by either increasing or decreasing the number of lipids in the outer leaflet (**Figure 2C**).

This structurally asymmetric response suggests that TREK-2 should also exhibit a functionally asymmetric response to the stretch induced by positive *vs*. negative pressure, and although their effects have been questioned (46), the functionally asymmetric effects of non-cylindrical lysolipids are consistent with this hypothesis. Nevertheless, direct functional studies of membrane curvature and leaflet asymmetry are experimentally challenging (6, 47), particularly with eukaryotic MS channels. Traditionally, pipette-based electrophysiological recordings are used in conjunction with the application of either positive or negative pressure to stretch the membrane. However, many different factors arising from the Ω shape of the membrane within the pipette and preferential adhesion of the outer leaflet to the glass complicate the interpretation of such experiments (6, 18, 48), and may have contributed to the different reported effects of negative *vs*. positive pressure on K2P channels (23, 24, 43). Therefore, we chose a more controlled approach and examined the mechanosensitivity of purified TREK-2 proteins reconstituted in a lipid bilayer system with a defined symmetrical composition and less complex geometry.

TREK-2 single channel activity in a planar lipid bilayer. In our previous studies, we have shown that a purified truncated version of TREK-2 retains its core functional properties, including its intrinsic mechanosensitivity, when reconstituted into a planar lipid bilayer (31, 34). For these experiments, we reconstituted TREK-2 into giant unilamellar vesicles (GUVs) and used a planar patch clamp system (see methods for details) (49). This has the advantage of a less complex geometry than pipette-based recordings and fewer of the complications that arise from the Gibbs plateau border in traditional BLMs.

However, one problem is that TREK-2 orients randomly when reconstituted into GUVs and this precludes any form of macroscopic analysis of membrane asymmetry. We therefore examined whether it was possible to measure responses to positive and negative pressure at the single channel level. **Figure 3A** shows a typical recording of these purified TREK-2 channels. Under these conditions (symmetrical 200 mM K^+, -80 mV), two main conductances were observed; one large conductance ~305 pS, and another ~155 pS. However, these arise from oppositely-oriented channels that possess an asymmetric unitary conductance. This rectification is more clearly observed in recordings of single channels that reveal only a single channel type with either the larger unitary conductance at negative potentials, or vice versa for a channel in the opposite orientation (**Figure 3B)**. A difference in channel activity is also seen at the equivalent of positive potentials with the smaller conductance exhibiting increased open probability and a less flickery behavior (see also **Supplementary Figs S1A-D**).

The single channel conductance of TREK-2 has been reported to vary dependent upon the length of the N-terminus, with shorter splice variants and truncations stabilizing a larger ~250 pS conductance with similar rectification (50, 51). Therefore, given the truncated N-terminus of the purified protein used in these studies, the single channel conductances we observe here (in 200 mM KCl) are entirely consistent with those expected for TREK-2. However, to confirm channel identity and orientation we made use of blockers known to inhibit TREK-2 from either the outside, or the inside of the membrane.

Tetrapentylammonium (TPA) blocks TREK-2 channels from the intracellular side by binding within the inner pore (52). By contrast, Ruthenium Red selectively blocks TREK-2 from the outside by binding just below the external CAP domain (53). To enable comparison of orientation and voltage with pipette-based recordings, we refer to channels oriented with their extracellular cap domain downward toward the glass chip as ‘inside-out’ (TREK-$2^{in/out}$), with the opposite orientation defined as ‘outside-out’ (TREK-$2^{out/out}$). Using this notation, we found that TPA only inhibited channel activity when applied from the equivalent of the inside, and that Ruthenium Red only inhibited

from the outside (**Figure 3C and 3D** and **Supplementary Fig S1E and S1F**). This therefore confirmed that these recordings represent TREK-2 inserted in opposite orientations, and that these different orientations can also be distinguished on the basis of their different unitary conductances.

Asymmetric mechanosensitivity of TREK-2. Previous models have suggested that a functionally asymmetric response to positive *vs*. negative pressures results from differences in stretch-induced membrane curvature and the resultant pressure profile asymmetry. This appears to be supported by the asymmetric action of lysolipids and the mechanosensitive toxin GsMTx4 on channel function (40, 42). However, the overall lateral tension within the membrane will increase in both leaflets when it is stretched by either negative or positive pressure. Therefore, if increased tension *per se* is sufficient to activate TREK-2, then the channel should be activated by both positive *and* negative pressure changes. However, if the asymmetric structure of the channel allows it to differentiate between changes in tension in the two leaflets then this will be orientation-dependent and may also produce a difference in its response to the different types of curvature induced by positive *vs.* negative pressures.

To examine this question, we applied either positive or negative pressure to bilayers containing a single TREK-2 channel. **Figure 4A** shows that an 'inside-out' channel is activated by an increase in negative pressure (-80 mbar), but when the same channel was exposed to an equivalent jump in positive pressure (+80 mbar) no equivalent activation was observed, instead there was a small decrease in activity. This functionally asymmetric response to different pressure changes between -120 and +120 mbar is shown in **Figure 4B**. Importantly, the opposite behavior was also seen in a single 'outside-out' channel.

Inverse asymmetric regulation of oppositely oriented channels. These results suggest that, under these particular recording conditions, the asymmetric changes in shape and cross-sectional area of TREK-2 are reflected in a functionally asymmetric response to changes in positive *vs* negative pressure. However, although these recordings are from purified proteins in GUVs using

a planar patch clamp configuration, the precise geometry and mechanics of these bilayers is unknown and they may already possess some form of inherent asymmetry that might account for this behavior.

To examine this further, we next studied the simultaneous behavior of two oppositely oriented channels within the same bilayer. In this important control experiment, if these two channels exhibit equally asymmetric (but inverse) responses to positive *vs.* negative pressure changes, then this effect is unlikely to result from any intrinsic artefacts in the recording system, e.g. curvature when the bilayer forms a Giga-Ohm seal on the glass chip, or preferential adhesion of a single leaflet to the glass surface. If any such intrinsic asymmetry exists within the recording system then it is unlikely that a channel in the opposite orientation would also exhibit the 'inverse' behavior, particularly if this behavior is seen simultaneously in two or more such oppositely oriented channels.

Fortunately, the asymmetric single channel conductance of TREK-2 makes it possible to distinguish between channels in opposite orientations. However, when more than one channel exists then openings of identical conductance can occur at the same time (e.g. **Figure 2A**). We therefore created an in-house analysis protocol to facilitate sorting of channel activity into contributions from either 'inside-out' or 'outside-out' channels (see **methods** and **supplementary information** for details).

Figure 5A shows how this approach can be used to analyze the pressure response in recordings that contain up to two channels of each orientation (see also **Supplementary Figure S2**). This reveals that in response to a step of -80 mbar, the 'inside-out 'channels become activated, whilst the oppositely-oriented 'outside-out' channels are not activated and exhibit a much smaller-fold decrease. By contrast, when the same channels are then exposed to +80 mbar, the exact opposite is seen: the outside-out channels become activated in preference to the inside-out channels. The relative responses of these oppositely oriented channels to steps between -120 and +120 mbar are shown in **Figure 5B**. This clearly demonstrates a functionally asymmetric

response with preferential activation by the equivalent of 'negative' pressure.

Stretch-activation preferentially destabilizes a closed state of the channel. Although both the Up and Down conformations of TREK-2 can be conductive, our previous studies show that stretch-activation preferentially stabilizes the Up conformation and that this has a positive allosteric effect on the filter gating mechanism (31, 33). However, the precise relationship between the different conformational states of any ion channel and their behavior at the single channel level is complex and not fully understood. Previous single-channel recordings of wild-type TREK-2 have been difficult to analyze because alternative translation initiation produces multiple isoforms with different conductance levels (51), but the purified TREK-2 protein studied here represents a single species with a well-behaved large conductance. We therefore examined the response of these single channels to stretch-activation in more detail.

The typical behavior of a single inside-out channel at -80 mV is shown in **Figure 6A**. Calculation of the open and closed dwell time distributions indicates they can be well fit with one main open time and three distinct closed times (**Figure 6B**). The application of membrane stretch increases the overall channel open-probability, but does not affect either the open dwell time, or the two shorter closed times (**Figure 6C)**. Instead, the increase in burst duration and open probability appears to arise through a selective reduction in the longest of the three closed times (**Figure 6D**) therefore suggesting a possible link between these structural and functional states.

Discussion

In this study, we have used a multidisciplinary approach to demonstrate that the mechanosensitive TREK-2 K^+ channel can detect a pressure profile asymmetry within a lipid bilayer membrane. Furthermore, we demonstrate that this asymmetric mechanosensitivity results from uneven changes in shape and cross-sectional area of the protein. This confers TREK-2 with the ability to sense a complex profile of forces across the membrane and it is likely to be critical

for the diversity of physico-mechanical coupling processes that mechanosensitive K2P channels are required to regulate.

Living organisms are able to perceive and respond to a diverse range of mechanical stimuli by utilizing a variety of mechanosensitive ion channels. Structures of the prokaryotic MscS/MscL channels have provided enormous insights into the underlying molecular mechanisms, but we have only recently obtained structures of some of the key eukaryotic mechanosensitive channels such the TREK/TRAAK family of K2P channels and the Piezo channels. The 'propeller like' curved arms and overall size of the Piezo channels immediately suggests possible mechanisms for sensing changes in membrane curvature, but current structures are of insufficient resolution for detailed studies (2, 54). By contrast, a large number of high resolution structures have now been determined for the TREK/TRAAK family, providing an excellent model system for how these MS channels move between their different conformations in response to membrane stretch.

For MS channels to exhibit the diversity of responses required to control so many different physiological process then they must be able to respond to a more complex profile of forces than just symmetrical changes in lateral tension. One such example is an ability to differentiate between changes in tension in individual leaflets of the bilayer i.e. to be able to detect a pressure profile asymmetry. Several thermodynamic descriptions of mechanosensitivity have proposed mechanisms by which this might occur. Amongst these is 'shape-sensitivity' whereby the change in cross-sectional area of the protein are different between the inner and outer leaflets.

Several of these ideas for asymmetric mechanosensitivity in K2P channels were proposed before their structures were solved (41), but until now direct evidence for this was either lacking or contradictory and may have resulted from differences in the recording systems used. A cautionary tale highlights many of the experimental challenges involved (6) and it is unlikely that our recording system is free of all geometric and/or mechanical artefacts. However, the ability to study the simultaneous inverse responses of oppositely-oriented channels provides a powerful argument against such artefacts being the origin of the functional asymmetry we observe.

It has been proposed that there are three basic types of structural deformation that underlie the thermodynamics of mechanosensitive channel gating (36): i) a symmetrical change in cross-sectional area within the plane of the membrane that responds to lateral tension; ii) a change in shape (without an overall change in area) that responds to differences in tension or 'torque' between the leaflets; and iii) a change in length that responds to hydrophobic mismatch. It is highly unlikely that these different mechanisms are mutually exclusive, but our previous study suggests hydrophobic mismatch is not sufficient *per se* to drive this structural transition in TREK-2 (34). In addition, these new results implicate a role for a combination of the other two mechanisms during TREK-2 mechanogating i.e. both a change in cross-sectional area and a change in shape.

The structural and functional response of these mechanosensitive TREK channels to a symmetrical change in the pressure profile is consistent with previous predictions for the required change in cross-sectional area (37). However, we now also provide evidence for the ability of these channels to detect a pressure profile asymmetry. The asymmetric structural changes in TREK-2 that underlie this response not only result from the need to maintain the integrity of the selectivity filter (35), but also the requirement to detect a wide variety of mechanical stimuli.

Symmetrical changes in the lateral pressure profile will elicit conformational changes in TREK-2 that are independent of channel orientation. However, when this asymmetric channel structure inserts into the membrane it has been shown to affect the local environment (i.e. pressure profile) differently in the outer *vs*. inner leaflets (34). Thus, although changes in global curvature *per se* are thought to be of negligible energetic consequence for MS channel activation, the direction of the curvature produced by positive vs negative pressure will be relevant because it has different effects on the two leaflets of the bilayer (19, 20, 55). Furthermore, many of the biologically-relevant mechanical forces which act on the membrane are unlikely to act equally on both leaflets and will also produce asymmetric effects on the pressure profile such as those shown in the cartoon in **Figure 7**. Similar effects may also result from different lipid compositions in the two

leaflets, and the inherent structural asymmetry of TREK-2 is therefore well-designed to detect any such pressure profile asymmetry that results from this.

Sensitivity to asymmetry within the pressure profile will endow these channels with the ability to focus the effects of different mechanical forces which act upon the membrane and to fine-tune cellular electrical responses accordingly. This functional diversity may also be further modified by the intracellular C-terminal domain that extends from M4. However, this domain is missing in the current crystal structures and no structural information currently exists, so it may be premature to speculate precisely how this domain might modulate the response of these channels to tension and/or curvature.

Our results also suggest other possible advantages of this planar patch-clamp bilayer recording system. In particular, the ability to obtain high-quality single channel recordings of TREK-2 channel activity may provide further insights into the relationship between channel structure and single channel activity during mechanogating. This recording system therefore represents an excellent opportunity for future studies in this area.

In summary, the results presented here provide compelling evidence for a versatile mechanism of sensing membrane tension by a eukaryotic MS ion channel that allows functional integration of a broad profile of membrane forces. These effects are not only consistent with its structurally asymmetric structural architecture, but also more representative of the complex sensory mechanisms that underlie its physiological role. The structures of other eukaryotic MS channels are also now becoming available and it will be interesting to examine how the mechanisms we describe here relate to the function of other mechanosensitive ion channels.

Materials and Methods

Molecular Dynamics. Increased bilayer tension results in an increase in the lateral area per lipid (APL) (34, 44). 'Asymmetric tension' was therefore simulated in each leaflet using an NPAT ensemble and creating mismatch in the lateral APL in either the outer or inner leaflet i.e. the simulation box size was fixed and the number of lipids in each leaflet was varied. In our previous study (34), the maximum P-50 stretch protocol increased the APL ~35%. We therefore used a lipid mismatch of 35% in the NPAT ensemble simulations to mimic these increases. To mimic a similar change in torque (without an increase in tension in the inner leaflet) lipids were added randomly into the outer leaflet by gradually increasing their number and energy minimisation to avoid an infinite force on the atom(s). The maximum mismatch in this case was limited to +16% to prevent bilayer distortion and instability. All-atom simulations of TREK-2 in these asymmetric bilayers were then run as before (34). Briefly, a 200 ns equilibrium NPT ensemble simulation of the TREK-2 'Down-state' (PDB: 4XDJ) was performed to obtain the equilibrium APL. The last frame was then used as the initial structure for 200 ns NPAT ensemble simulations after randomly removing (or adding) lipids in the relevant leaflet. Simulations were repeated with different randomly removed lipids and random velocities. All simulations were performed with GROMACS 4.6 (56), Charmm36 force field (57) and a 2 fs integration time step. Each simulation contained about 200 lipids, 25,000 TIP3P water molecules and 150 mM KCl. Semi-isotropic pressure was controlled using a Parrinello-Rahman barostat (58) with a compressibility of 0 in the *x-y* plane and 4.5×10^{-5} bar^{-1} in the *z* direction. Lateral pressure profiles were calculated as before (34).

Preparation of TREK-2 and GUVs. The human TREK-2 (*KCNK10*) 'crystal construct' protein (Gly^{67} to Glu^{340}) was expressed and purified as previously described (26). Briefly, 1,2-diphytanoyl-sn-glycero-3-phosphocholine (DPhPC) was dissolved in chloroform to a concentration of 10 mM and stored at -20°C. The GUVs where then made by electroformation in 1 M sorbitol using the Vesicle Prep Pro (Nanion Technologies, GmbH). Purified TREK-2 was then mixed with GUVs to a final concentration of ~1 - 5 µg/ml and incubated overnight at 4 °C with Bio-Beads prior to use.

Bilayer recordings*.* All electrophysiological recordings were performed with the Nanion Port-a-Patch planar patch-clamp system connected to an Axopatch 200B amplifier via a Digidata 1440A digitizer (Molecular Devices). The microstructured apertures in the glass chips of this planar patch clamp system are used to form Giga-Ohm seals on TREK2-containing GUVs which burst upon contact with the glass surface (49). All data was filtered at 10 kHz and recorded at a 250 kHz sampling rate. Experiments were carried out in symmetrical 200 mM KCl, 10 mM HEPES pH 6.0 solutions. Channel open probability (Po) was evaluated over 5 second periods before and after each stated pressure jump. Data from single channel patches were idealized in MATLAB with a half-amplitude threshold crossing algorithm and a 43 µs resolution was imposed before distributions were calculated using the maximum likelihood method. The critical time for classification of bursts was found by numerically solving: $1\text{-}e^{-tc/tm} = e^{-tc/tl}$ for *tc*, where *tm* and *tl* are the intermediate and long closed dwell times, respectively (59). Plots and statistical analysis were performed with GraphPad Prism 5 software. Procedures for the analysis of channel activity based on orientation are described below with further description in the supplementary information.

Single channel sorting protocol*.* The voltage dependence of the single channel properties of TREK2 allows dissection of channel orientation. To achieve this a custom MATLAB analysis protocol was created that facilitates sorting of channel activity into contributions from TREK-$2^{In/Out}$ and TREK-$2^{Out/Out}$ channels (**Supplementary Figure S2**). Multiple channel activity is sorted into clusters (based on signal amplitude) that represent possible channel combinations and then joined together (brief deflections below the threshold limits are thus excluded). After removal of clusters shorter than 40 µs, overlapping prospective channel combinations are evaluated and classified based on a set of parameters that include *closure frequency, slope evaluation* (sum of slope evaluation points/cluster length) (**Supplementary Figure S2C**), *ideal TREK-*$2^{In/Out}$ (frequency of fast 28-32 pA amplitude jumps/cluster length) and *immediate neighbour* signals. The rationale behind the immediate neighbouring signals is that a fast transition between different cluster categories should be as simple as possible, i.e. a single channel opening or closing is

more likely than two channels opening and/or closing simultaneously.

A key feature of the script is the ability to distinguish one TREK-$2^{In/Out}$ from two simultaneously opened TREK-$2^{Out/Out}$ channels which have similar combined amplitude. To validate this approach, we evaluated 30 sec recordings of patches with either two TREK-$2^{In/Out}$ or two TREK-$2^{Out/Out}$ channels. In a 30 sec recording of a bilayer with two TREK-$2^{In/Out}$ channels, the script successfully identified 94.2 % of the activity as being from TREK-$2^{In/Out}$ while 1.8 % was wrongly categorized as TREK-$2^{Out/Out}$. When a bilayer with two TREK-$2^{Out/Out}$ channels was evaluated for 30 seconds the script correctly identified 96.9 % of the signals as TREK-$2^{Out/Out}$, misinterpreted 0.1 % as TREK-$2^{In/Out}$ and missed 3 % (see also **Supplementary Figure S2**). The MATLAB script for channel sorting is available at: https://github.com/biologichael/Channel-sorting

Acknowledgements

We thank the many members of our laboratories who have discussed these results with us. In particular, we thank Jackie Ang for his help with providing samples of the TREK-2 protein. This work was funded by grants to S.J.T, M.S.P.S and E.P.C from the Wellcome Trust and the BBSRC. M.V.C was supported by fellowships from the Carlsberg and Lundbeck Foundations, and V.J. by a Thai Government Scholarship. EPC is a member of the SGC, a registered charity (1097737) that receives funds from AbbVie, Bayer Pharma AG, Boehringer Ingelheim, the Canada Foundation for Innovation, Genome Canada, GlaxoSmithKline, Janssen, Lilly Canada, Merck & Co., the Novartis Research Foundation, the Ontario Ministry of Economic Development and Innovation, Pfizer, São Paulo Research Foundation-FAPESP, Takeda, EU/EFPIA Innovative Medicines Initiative (IMI) Joint Undertaking and the Wellcome Trust.

Conflict of Interest

The authors declare that they have no conflict of interest.

Figure Legends

Figure 1. Asymmetric structural changes in response to membrane stretch. (**A**) The TREK-2 (Down-state) K2P channel structure embedded within a lipid bilayer. Only the TM helices (M1-M4) are colored. (**B**) Overlay of surface representations of the Down (grey) and Up (red) conformations of the channel to illustrate the difference in cross-sectional area of the two conformations. Note that most of the structural changes are seen in the lower half of the protein. (**C**) As previously reported (34), these asymmetric changes are seen more clearly in this comparison of the stretch-induced change in cross-sectional area. (**D**) The cross-sectional area that TREK-2 assumes within the bilayer can also be considered as a funnel shape. Upon membrane stretch (red) the lower half expands and the overall structure becomes more symmetrical. The upper half of the protein remains relatively constant in order to maintain the structural integrity of the selectivity filter.

Figure 2. Structural changes in TREK-2 induced by pressure profile asymmetry. (**A**) The NPAT simulation method used to produce asymmetric changes in tension. The area of the bilayer is kept constant (simulation box shown in black) and lipids randomly removed from either the inner or outer leaflet to increase the area per lipid in that leaflet. Left: structure of the down state before lipid removal. Right; structure after tension is increased only in the inner leaflet. Orange spheres represent the lipid headgroups and shading relates to lipid density. Note this protocol does not distort the bilayer. (**B**) Pressure profile asymmetry induced by removal of lipids from the inner leaflet (blue). A symmetrical unstretched bilayer is shown in black and reveals major changes in tension in the inner leaflet and pressure profile asymmetry across the bilayer. (**C**) Left: RMSD comparison of the simulated TREK-2 Down-state structure vs the Up-state crystal structure. When tension is selectively increased in the lower leaflet by removal of lipids, the Down-state quickly moves towards the Up-state (blue). However, when tension is increased only in the outer leaflet (black) by lipid removal there is no movement towards the Up-state. Also no movement is seen if the number of lipids is increased in the outer leaflet alone suggesting that a

change in torque alone is not sufficient. Right: overlay of the simulated structures after 200 ns with the 'up state' structure induced by symmetrical stretch (34).

Figure 3. Recording of single TREK-2 channels in a planar lipid bilayer. (**A**) Single channel recordings of purified TREK-2 channels in an unstretched planar patch-clamp lipid bilayer. Cartoon of how the channel randomly incorporates in either the 'inside-out' (green) or 'outside-out' orientation (red). Inset is shown a recording from a bilayer with two oppositely oriented channels. (**B**) Two types of single channel activity are observed denoted TREK-$2^{in/out}$ or TREK-$2^{out/out}$. These opposite orientations can be distinguished based upon their rectification. Left: single TREK-$2^{in/out}$ channel with lower (~155 pS) conductance and long openings at +80 mV, but higher (~305 pS) conductance and flickery openings at -80 mV (see also **Figure S1A**). Right: single TREK-$2^{out/out}$ channels exhibit the opposite characteristics. (**C**) Confirmation of orientation with specific blockers: Tetrapentylammonium blocks TREK-2 from the inside at a site within the inner cavity. A bilayer with at least four TREK-$2^{in/out}$ channels is blocked when TPA is applied from the equivalent of the inside. (**D**) By contrast, Ruthenium Red blocks at a site within the outer mouth of the pore, just below the CAP domain. This bilayer contains at least two TREK-$2^{out/out}$ channels, which are blocked by the addition of Ruthenium Red from the equivalent of the outside. Control experiments in the reverse orientation for each blocker are shown in **Figure S1B**.

Figure 4. Asymmetric response to positive vs. negative pressure. (**A**) Bilayers with single channels in either the inside-out (left) or outside-out orientation (right) were stimulated by pressure jumps from 0 to +/- 80 mbar. The pump used to apply pressure is positioned underneath the bilayer and the direction of the pressure change on the bilayer is shown by the arrows. (**B**) The mean $\log_{10}$ fold fold-change in Po for each channel orientation is shown in response to a variety of pressure changes from -120 to +120 mbar. The values above each error bar indicate the number of independent replicates and error bars represent SEM. Asterisks represent significance of difference between the two orientations at opposite pressures: ***P≤0.001, **P≤0.01, *P≤0.05 (two-way unpaired t-tests). Note that whilst negative pressure activates inside-out channels, the

outside-out channels are preferentially activated by positive pressure (i.e. the equivalent of negative pressure for inside-out channels).

Figure 5. Inverse regulation of oppositely orientated channels. Simultaneous recording of bilayers with at least one channel of each orientation, and up to a maximum of two of each. (**A**) Example of change in channel currents in response to either positive or negative pressure (recording at -80 mV). The colour chart is the result of our in-house analysis used to classify channels according to their orientation. (**B**) The mean $\log_{10}$ fold-change in Po for these oppositely oriented channels is shown in response to a variety of pressure changes from -120 to +120 mbar. The values above each error bar indicate the number of independent replicates and error bars represent SEM. Asterisks represent significance of difference between the two orientations: ***P≤0.001, **P≤0.01, *P≤0.05 (two-way unpaired t-tests). Note that whilst negative pressure activates only inside-out channels (green), only positive pressures activate outside-out channels (red) i.e. the equivalent of negative pressure for inside-out channels.

Figure 6. Selective effect of pressure activation on the long closed state of TREK-2. (**A**) Representative segment of a single TREK-$2^{in/out}$ channel recording with a burst expanded as indicated by the arrows. (**B**) Maximum likelihood fits to open, closed and burst dwell time distributions from an unstretched bilayer at 0 mbar. (**C-D**) Same, but recorded after a pressure jump to -80 mbar. Note the selective reduction in the long closed time (black arrow).

Figure 7. Response of TREK-2 to an asymmetric pressure profile. This cartoon illustrates a model for how TREK-2 detects a pressure profile asymmetry. In order to maintain the structural integrity of the selectivity filter, stretch-induced expansion occurs primarily within the lower leaflet. This 'shape sensitivity' means that the channel can detect an asymmetry increase in tension such as that induced by membrane curvature or other asymmetric forces and when analysed in a bilayer, these responses will be orientation dependent. Overall, such asymmetric functional responses will allow these MS channels to focus the effects of different mechanical forces and to fine-tune cellular electrical responses accordingly.

References

1. Katta S, Krieg M, & Goodman MB (2015) Feeling force: physical and physiological principles enabling sensory mechanotransduction. *Annu Rev Cell Dev Biol* 31:347-371.
2. Ranade SS, Syeda R, & Patapoutian A (2015) Mechanically Activated Ion Channels. *Neuron* 87(6):1162-1179.
3. Sukharev S & Sachs F (2012) Molecular force transduction by ion channels: diversity and unifying principles. *J Cell Sci* 125(Pt 13):3075-3083.
4. Anishkin A, Loukin SH, Teng J, & Kung C (2014) Feeling the hidden mechanical forces in lipid bilayer is an original sense. *Proc Natl Acad Sci U S A* 111(22):7898-7905.
5. Teng J, Loukin S, Anishkin A, & Kung C (2015) The force-from-lipid (FFL) principle of mechanosensitivity, at large and in elements. *Pflugers Arch* 467(1):27-37.
6. Sachs F (2015) Mechanical transduction by ion channels: A cautionary tale. *World J Neurol* 5(3):74-87.
7. Levina N*, et al.* (1999) Protection of Escherichia coli cells against extreme turgor by activation of MscS and MscL mechanosensitive channels: identification of genes required for MscS activity. *EMBO J* 18(7):1730-1737.
8. Booth IR & Blount P (2012) The MscS and MscL families of mechanosensitive channels act as microbial emergency release valves. *J Bacteriol* 194(18):4802-4809.
9. Martinac B, Adler J, & Kung C (1990) Mechanosensitive ion channels of E. coli activated by amphipaths. *Nature* 348(6298):261-263.
10. Pliotas C & Naismith JH (2016) Spectator no more, the role of the membrane in regulating ion channel function. *Curr Opin Struct Biol* 45:59-66.
11. Cantor RS (1997) Lateral Pressures in Cell Membranes: A Mechanism for Modulation of Protein Function. *The Journal of Physical Chemistry B* 101(10):1723-1725.
12. Cantor RS (1999) Lipid composition and the lateral pressure profile in bilayers. *Biophys J* 76(5):2625-2639.
13. Marsh D (2007) Lateral pressure profile, spontaneous curvature frustration, and the incorporation and conformation of proteins in membranes. *Biophys J* 93(11):3884-3899.
14. Gullingsrud J & Schulten K (2004) Lipid bilayer pressure profiles and mechanosensitive channel gating. *Biophys J* 86(6):3496-3509.
15. Zhang XC, Liu Z, & Li J (2016) From membrane tension to channel gating: A principal energy transfer mechanism for mechanosensitive channels. *Protein Sci* 25(11):1954-1964.
16. Reeves D, Ursell T, Sens P, Kondev J, & Phillips R (2008) Membrane mechanics as a probe of ion-channel gating mechanisms. *Phys Rev E Stat Nonlin Soft Matter Phys* 78(4 Pt 1):041901.
17. Deserno M (2015) Fluid lipid membranes: from differential geometry to curvature stresses. *Chem Phys Lipids* 185:11-45.
18. Bavi N*, et al.* (2014) Biophysical implications of lipid bilayer rheometry for mechanosensitive channels. *Proc Natl Acad Sci U S A* 111(38):13864-13869.

19. Bavi O*, et al.* (2016) Influence of Global and Local Membrane Curvature on Mechanosensitive Ion Channels: A Finite Element Approach. *Membranes (Basel)* 6(1).
20. Bavi O, Vossoughi M, Naghdabadi R, & Jamali Y (2016) The Combined Effect of Hydrophobic Mismatch and Bilayer Local Bending on the Regulation of Mechanosensitive Ion Channels. *PLoS One* 11(3):e0150578.
21. Pereira V*, et al.* (2014) Role of the TREK2 potassium channel in cold and warm thermosensation and in pain perception. *Pain* 155(12):2534-2544.
22. Renigunta V, Schlichthorl G, & Daut J (2015) Much more than a leak: structure and function of K2P-channels. *Pflugers Arch* 467(5):867-894.
23. Berrier C*, et al.* (2013) The purified mechanosensitive channel TREK-1 is directly sensitive to membrane tension. *J Biol Chem* 288(38):27307-27314.
24. Brohawn SG, Su Z, & MacKinnon R (2014) Mechanosensitivity is mediated directly by the lipid membrane in TRAAK and TREK1 K+ channels. *Proc Natl Acad Sci U S A* 111(9):3614-3619.
25. Peyronnet R, Nerbonne JM, & Kohl P (2016) Cardiac Mechano-Gated Ion Channels and Arrhythmias. *Circ Res* 118(2):311-329.
26. Garry A*, et al.* (2007) Altered acetylcholine, bradykinin and cutaneous pressure-induced vasodilation in mice lacking the TREK1 potassium channel: the endothelial link. *EMBO Rep* 8(4):354-359.
27. Bittner S*, et al.* (2013) Endothelial TWIK-related potassium channel-1 (TREK1) regulates immune-cell trafficking into the CNS. *Nat Med* 19(9):1161-1165.
28. Peyronnet R*, et al.* (2012) Mechanoprotection by polycystins against apoptosis is mediated through the opening of stretch-activated K(2P) channels. *Cell Rep* 1(3):241-250.
29. Brohawn SG, Campbell EB, & MacKinnon R (2013) Domain-swapped chain connectivity and gated membrane access in a Fab-mediated crystal of the human TRAAK K+ channel. *Proc Natl Acad Sci U S A* 110(6):2129-2134.
30. Brohawn SG, del Marmol J, & MacKinnon R (2012) Crystal structure of the human K2P TRAAK, a lipid- and mechano-sensitive K+ ion channel. *Science* 335(6067):436-441.
31. Dong YY*, et al.* (2015) K2P channel gating mechanisms revealed by structures of TREK-2 and a complex with Prozac. *Science* 347(6227):1256-1259.
32. Lolicato M*, et al.* (2017) K2P2.1 (TREK-1)-activator complexes reveal a cryptic selectivity filter binding site. *Nature* 547(7663):364-368.
33. McClenaghan C*, et al.* (2016) Polymodal activation of the TREK-2 K2P channel produces structurally distinct open states. *J Gen Physiol* 147(6):497-505.
34. Aryal P*, et al.* (2017) Bilayer-Mediated Structural Transitions Control Mechanosensitivity of the TREK-2 K2P Channel. *Structure* 25:708-718.
35. Nematian-Ardestani E, Jarerattanachat V, Aryal P, Sansom MSP, & Tucker SJ (2017) The Effects of Stretch Activation on Ionic Selectivity of the TREK-2 K2P K^+ Channel. *Channels (Austin)*: doi: 10.1080/19336950.2017.1356955
36. Markin VS & Sachs F (2004) Thermodynamics of mechanosensitivity. *Phys Biol* 1(1-2):110-124.

37. Maksaev G, Milac A, Anishkin A, Guy HR, & Sukharev S (2011) Analyses of gating thermodynamics and effects of deletions in the mechanosensitive channel TREK-1: comparisons with structural models. *Channels (Austin)* 5(1):34-42.
38. Frolov VA, Shnyrova AV, & Zimmerberg J (2011) Lipid polymorphisms and membrane shape. *Cold Spring Harb Perspect Biol* 3(11):a004747.
39. Yoo J & Cui Q (2009) Curvature generation and pressure profile modulation in membrane by lysolipids: insights from coarse-grained simulations. *Biophys J* 97(8):2267-2276.
40. Maingret F, Patel AJ, Lesage F, Lazdunski M, & Honore E (2000) Lysophospholipids open the two-pore domain mechano-gated K(+) channels TREK-1 and TRAAK. *J Biol Chem* 275(14):10128-10133.
41. Dedman A*, et al.* (2009) The mechano-gated K(2P) channel TREK-1. *Eur Biophys J* 38(3):293-303.
42. Gottlieb PA & Sachs F (2009) The Peptide GsMTx4 Inhibits the TREK-1 Channel from the Intracellular Side. *Biophysical Journal* 96(3 Supplement 1):255a.
43. Maingret F, Fosset M, Lesage F, Lazdunski M, & Honore E (1999) TRAAK is a mammalian neuronal mechano-gated K+ channel. *J Biol Chem* 274(3):1381-1387.
44. Markin VS & Sachs F (2015) Free Volume in Membranes: Viscosity or Tension? *Open J Biophys* 5(3):80-83.
45. Markin VS & Martinac B (1991) Mechanosensitive ion channels as reporters of bilayer expansion. A theoretical model. *Biophys J* 60(5):1120-1127.
46. Mukherjee N*, et al.* (2014) The activation mode of the mechanosensitive ion channel, MscL, by lysophosphatidylcholine differs from tension-induced gating. *FASEB J* 28(10):4292-4302.
47. Sachs F (2010) Stretch-activated ion channels: what are they? *Physiology (Bethesda)* 25(1):50-56.
48. Slavchov RI, Nomura T, Martinac B, Sokabe M, & Sachs F (2014) Gigaseal mechanics: creep of the gigaseal under the action of pressure, adhesion, and voltage. *J Phys Chem B* 118(44):12660-12672.
49. Sondermann M, George M, Fertig N, & Behrends JC (2006) High-resolution electrophysiology on a chip: Transient dynamics of alamethicin channel formation. *Biochim Biophys Acta* 1758(4):545-551.
50. Kang D, Choe C, Cavanaugh E, & Kim D (2007) Properties of single two-pore domain TREK-2 channels expressed in mammalian cells. *J Physiol* 583(Pt 1):57-69.
51. Simkin D, Cavanaugh EJ, & Kim D (2008) Control of the single channel conductance of K2P10.1 (TREK-2) by the amino-terminus: role of alternative translation initiation. *J Physiol* 586(Pt 23):5651-5663.
52. Piechotta PL*, et al.* (2011) The pore structure and gating mechanism of K2P channels. *EMBO J* 30(17):3607-3619.
53. Braun G, Lengyel M, Enyedi P, & Czirjak G (2015) Differential sensitivity of TREK-1, TREK-2 and TRAAK background potassium channels to the polycationic dye ruthenium red. *Br J Pharmacol* 172(7):1728-1738.
54. Syeda R*, et al.* (2016) Piezo1 Channels Are Inherently Mechanosensitive. *Cell Rep* 17(7):1739-1746.
55. Nomura T, Cox CD, Bavi N, Sokabe M, & Martinac B (2015) Unidirectional incorporation of a bacterial mechanosensitive channel into liposomal membranes. *FASEB J* 29(10):4334-4345.

56. Hess B, Kutzner C, van der Spoel D, & Lindahl E (2008) GROMACS 4: Algorithms for Highly Efficient, Load-Balanced, and Scalable Molecular Simulation. *J Chem Theory Comput* 4(3):435-447.
57. Best RB*, et al.* (2012) Optimization of the additive CHARMM all-atom protein force field targeting improved sampling of the backbone phi, psi and side-chain chi(1) and chi(2) dihedral angles. *J Chem Theory Comput* 8(9):3257-3273.
58. Bussi G, Donadio D, & Parrinello M (2007) Canonical sampling through velocity rescaling. *J Chem Phys* 126(1):014101.
59. Colquhoun D & Sakmann B (1985) Fast events in single-channel currents activated by acetylcholine and its analogues at the frog muscle end-plate. *J Physiol* 369:501-557.

/body

Figure 1

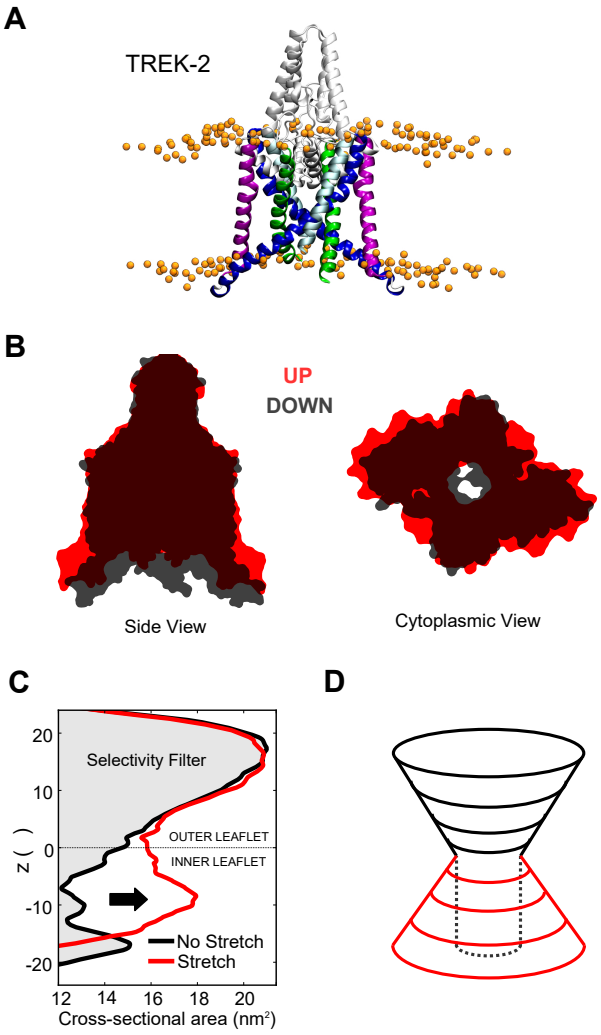
A
TREK-2
B
UP
DOWN
Side View
Cytoplasmic View
C
D
Selectivity Filter
OUTER LEAFLET
INNER LEAFLET
No Stretch
Stretch
z ( )
20
10
0
-10
-20
12
14
16
18
20
Cross-sectional area (nm²)

Figure 2

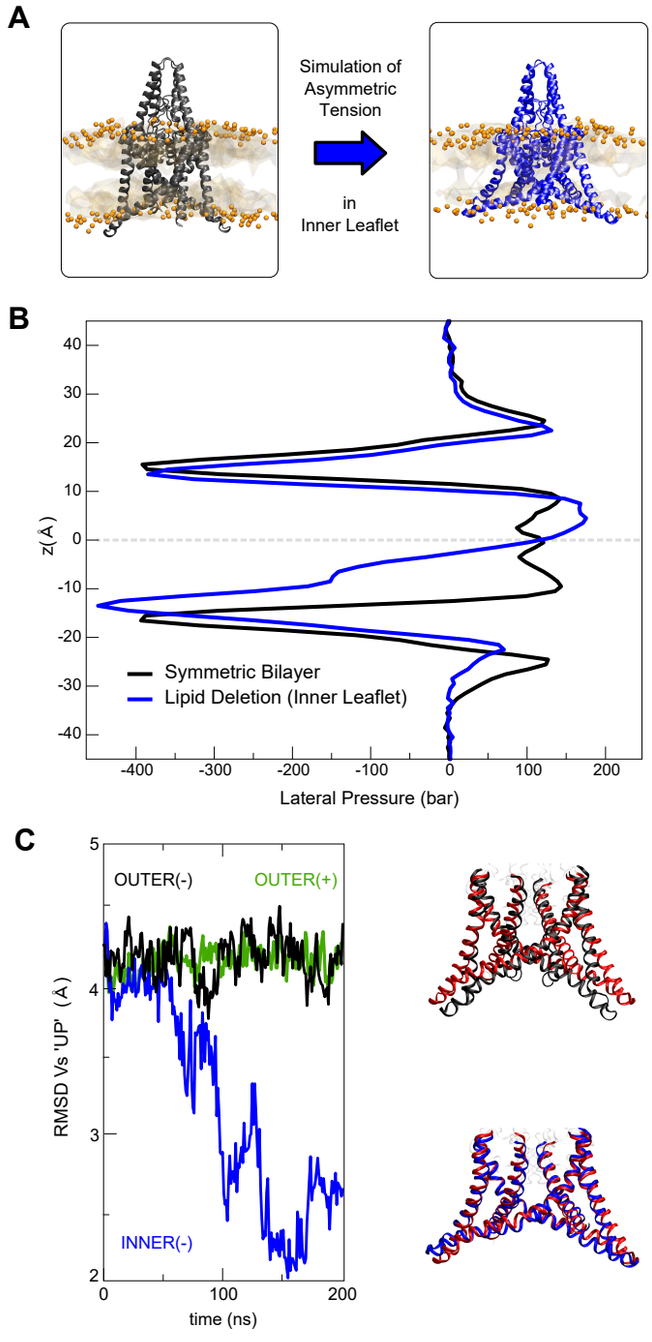
A
Simulation of
Asymmetric
Tension
in
Inner Leaflet
B
z(Å)
Symmetric Bilayer
Lipid Deletion (Inner Leaflet)
Lateral Pressure (bar)
C
OUTER(-)
OUTER(+)
INNER(-)
RMSD Vs 'UP' (Å)
time (ns)

Figure 3

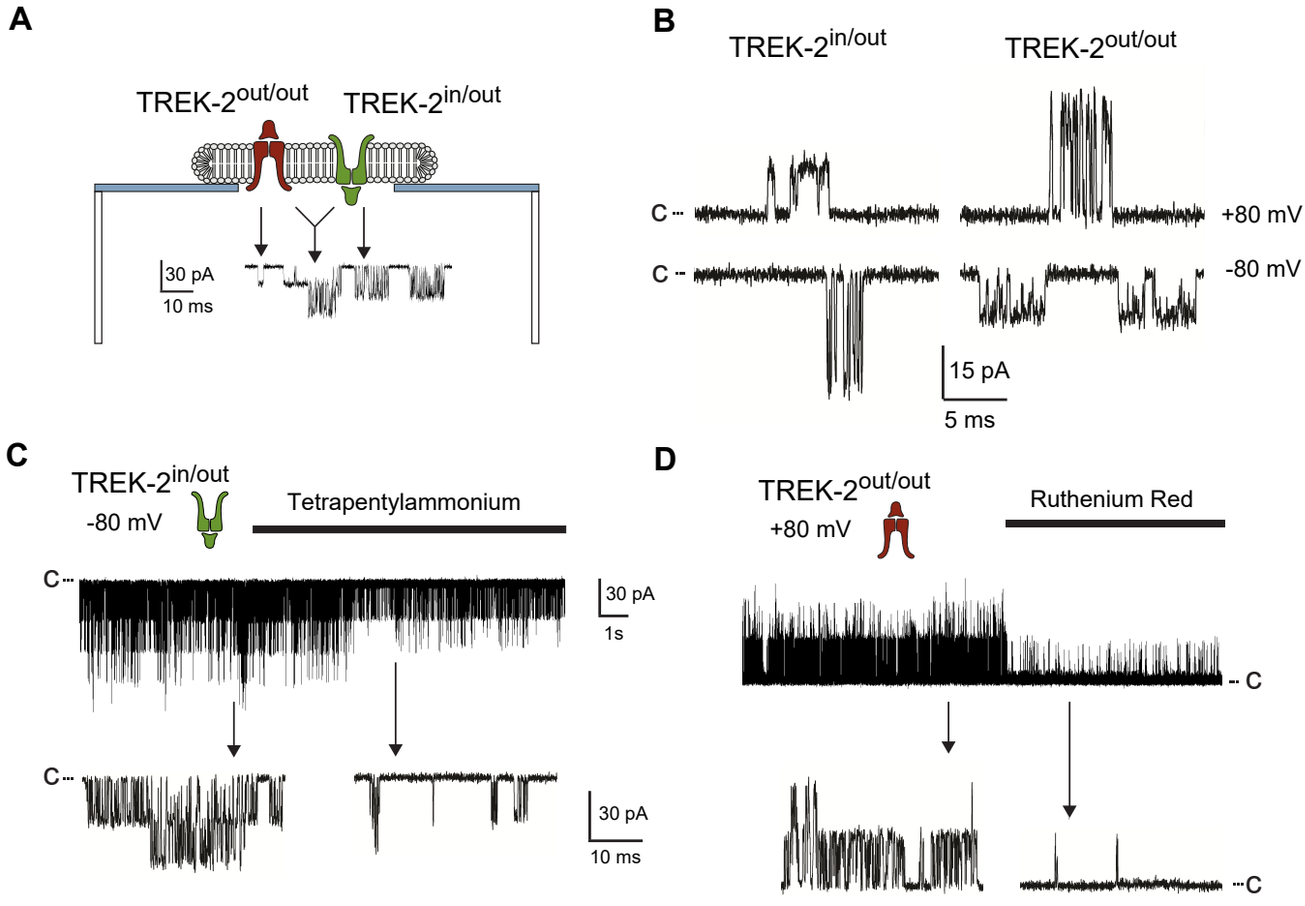
A
TREK-2out/out
TREK-2in/out
30 pA
10 ms
B
TREK-2in/out
TREK-2out/out
C
C
+80 mV
-80 mV
15 pA
5 ms
C
TREK-2in/out
-80 mV
Tetrapentylammonium
C
30 pA
1s
C
30 pA
10 ms
D
TREK-2out/out
+80 mV
Ruthenium Red
C
C

Figure 4

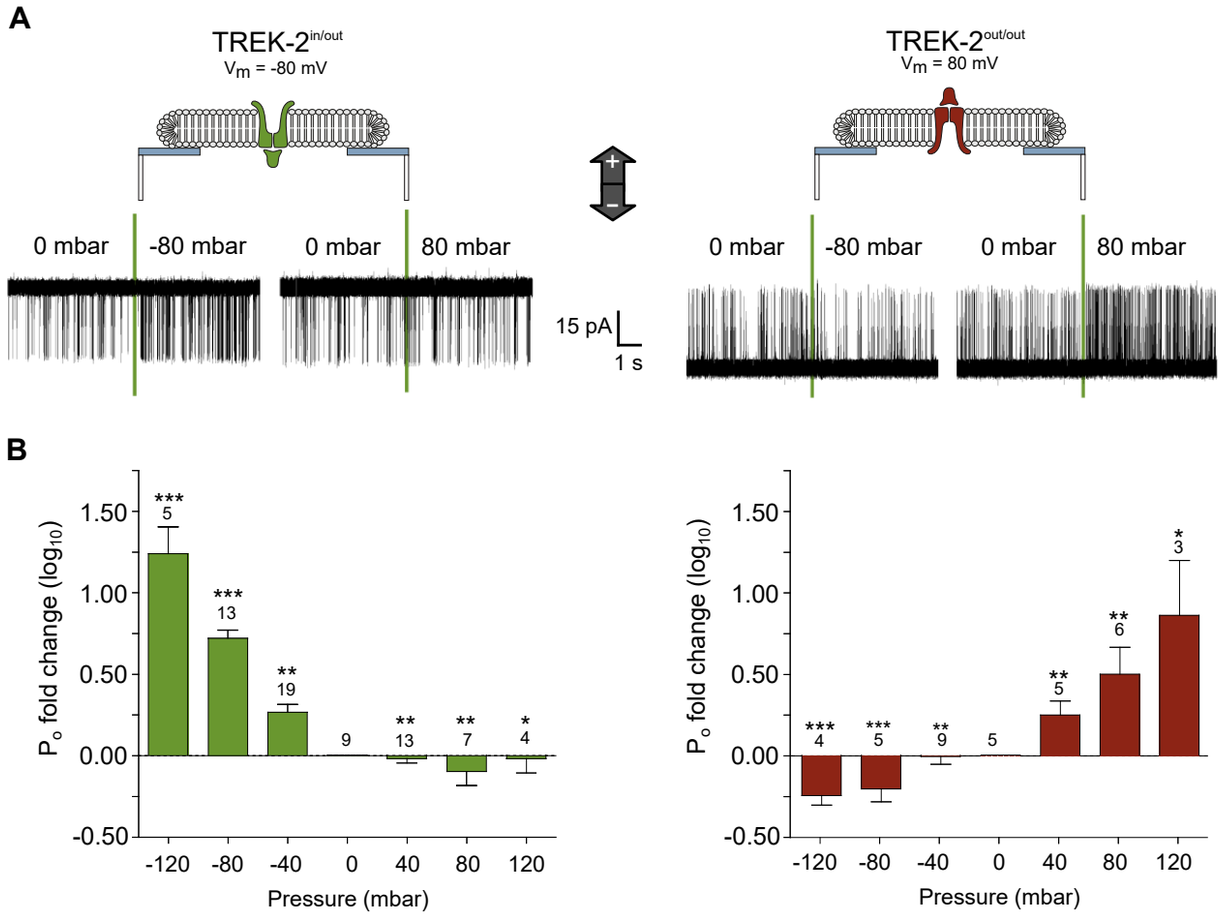
A
TREK-2in/out
Vm = -80 mV
TREK-2out/out
Vm = 80 mV
0 mbar
-80 mbar
0 mbar
80 mbar
15 pA
1 s
B
Po fold change (log10)
Pressure (mbar)
-120
-80
-40
0
40
80
120
1.50
1.00
0.50
0.00
-0.50

Figure 5

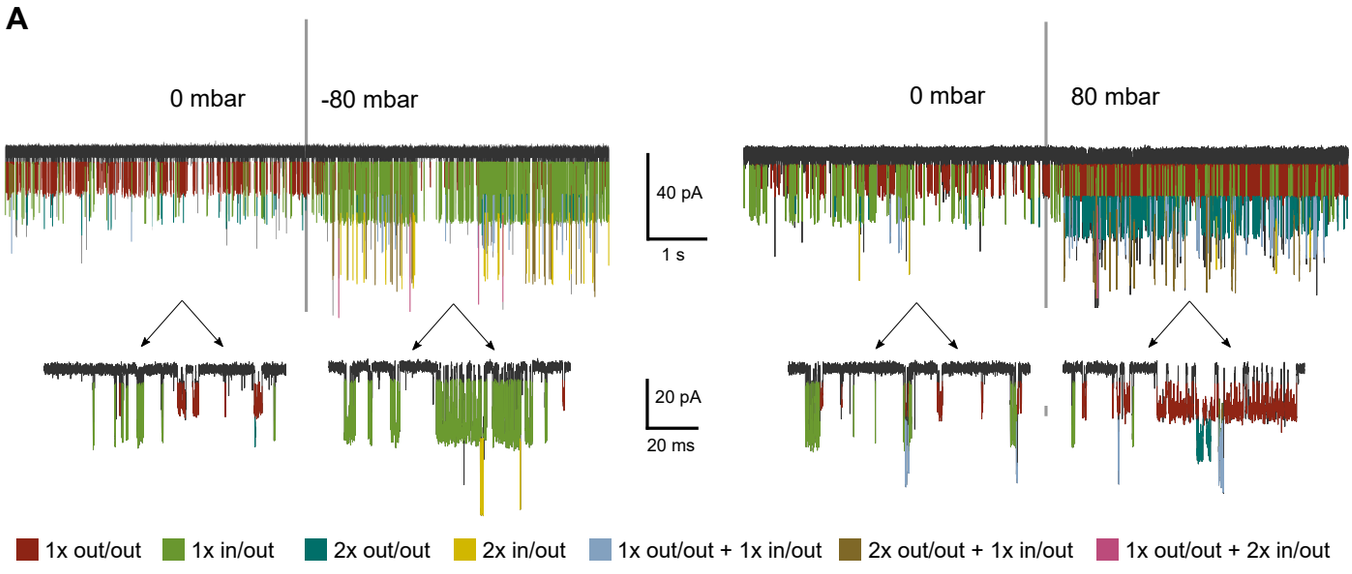
A
0 mbar
-80 mbar
0 mbar
80 mbar
40 pA
1 s
20 pA
20 ms
1x out/out
1x in/out
2x out/out
2x in/out
1x out/out + 1x in/out
2x out/out + 1x in/out
1x out/out + 2x in/out

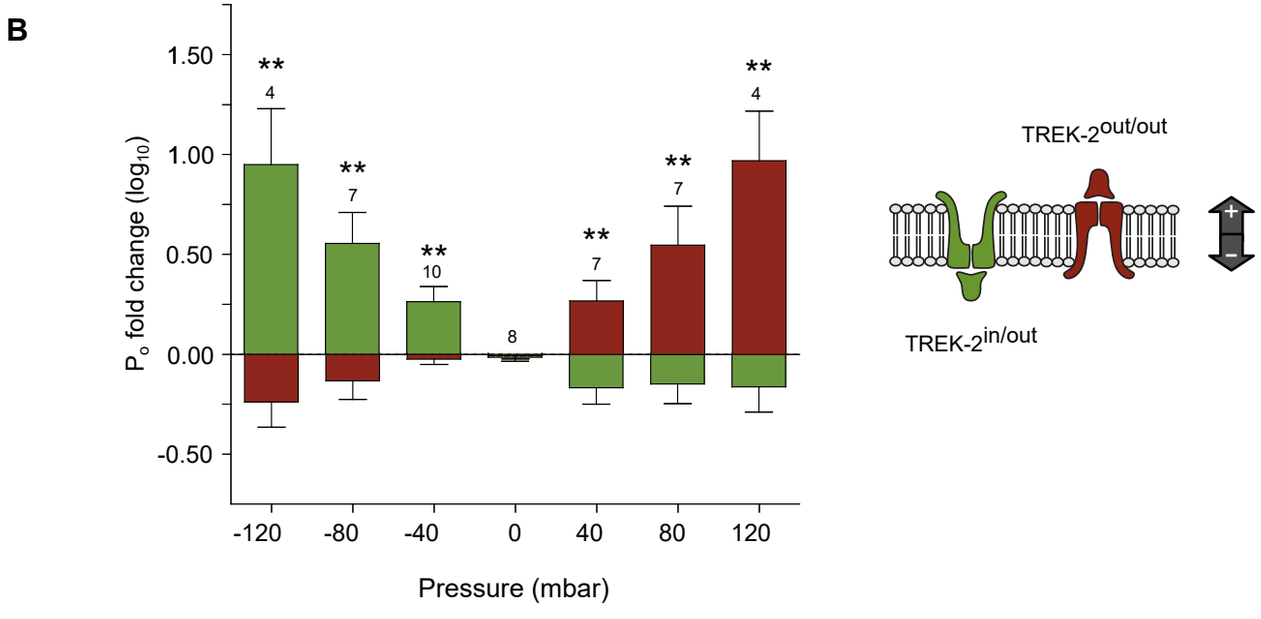
B
1.50
1.00
0.50
0.00
-0.50
P_o fold change (log_{10})
**
4
**
7
**
10
8
**
7
**
7
**
4
-120
-80
-40
0
40
80
120
Pressure (mbar)
TREK-2out/out
TREK-2in/out
+
−

Figure 6

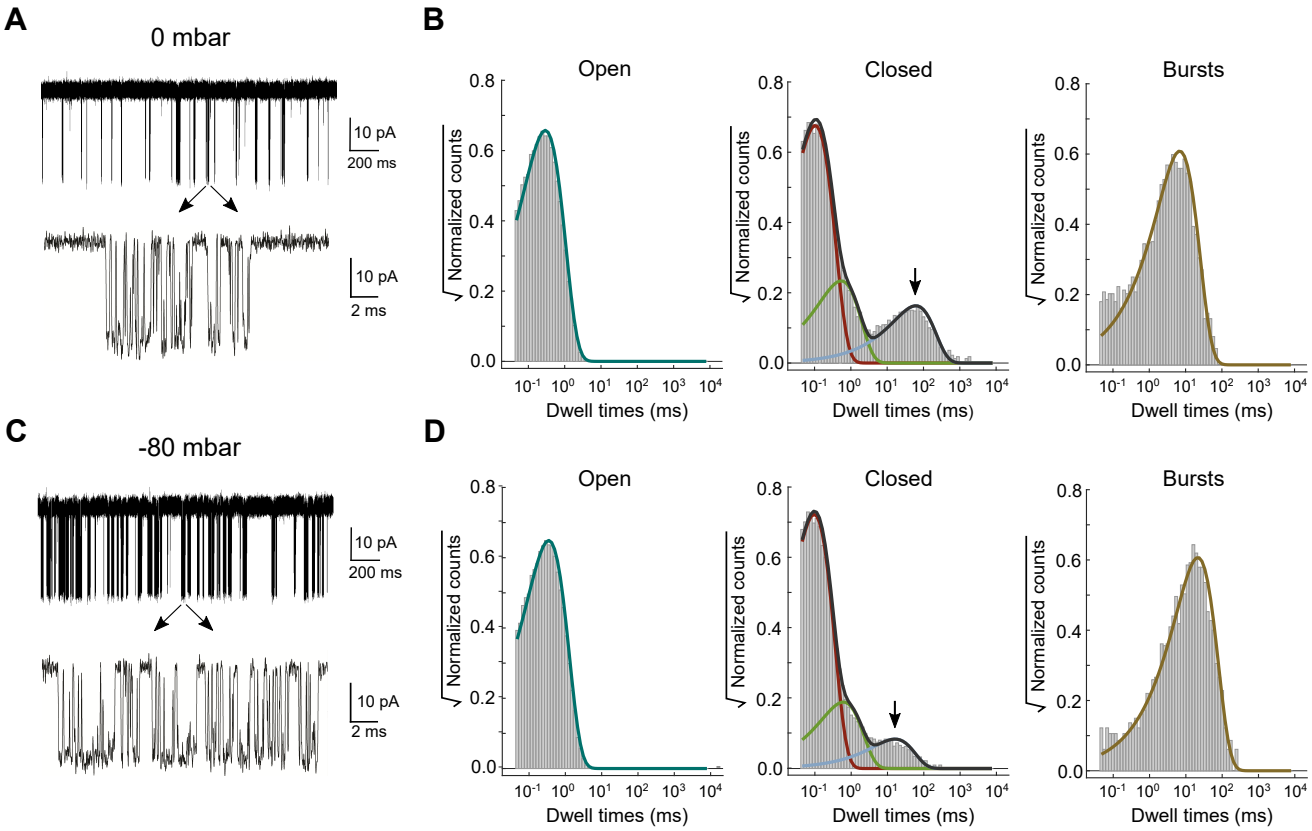
A
0 mbar
10 pA
200 ms
10 pA
2 ms
B
Open
Closed
Bursts
Normalized counts
Dwell times (ms)
C
-80 mbar
10 pA
200 ms
10 pA
2 ms
D
Open
Closed
Bursts
Normalized counts
Dwell times (ms)

Figure 7

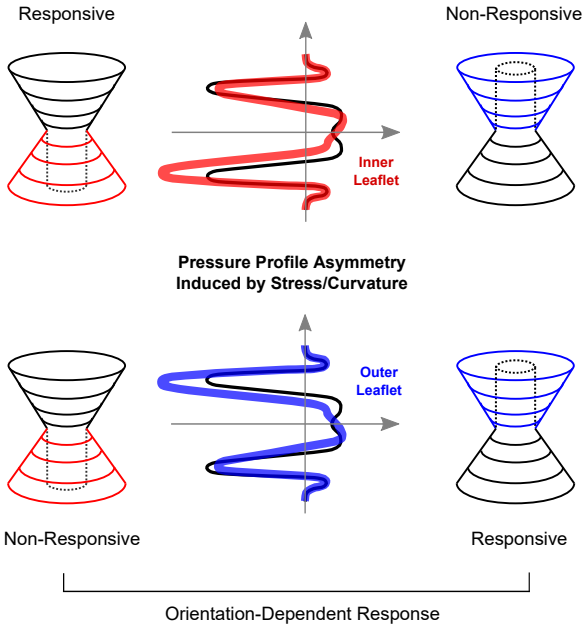
Responsive
Non-Responsive
Inner
Leaflet
Pressure Profile Asymmetry
Induced by Stress/Curvature
Outer
Leaflet
Non-Responsive
Responsive
Orientation-Dependent Response

Supplementary Figure Legends

Clausen et al. Asymmetric Mechanosensitivity in a Eukaryotic Ion Channel

Supplementary Figure S1 (related to **Figure 3**). **TREK-2 single channel characteristics and orientation**. (**A**) I/V plot showing that the single channel conductance of TREK-$2^{in/out}$ channels exhibit voltage-dependent rectification. (**B**) Voltage-dependence of the open probability for the same channels. (**C**) Plot highlighting the rectification seen in the conductance of single 'inside-out' channels recorded at +80 mV and -80 mV, and the inverse relationship for single 'outside-out' channels. (**D**) Inside-out channels exhibit a higher open-probability at positive potentials compared to negative potentials. The inverse relationship is seen for single outside-out channels. All data represent mean ± SEM (*n*=4) (**E**). TREK-$2^{in/out}$ channels are unaffected by Ruthenium Red (10 µM) applied from the equivalent of the inside (**F**) TREK-$2^{out/out}$ channels are not inhibited by Tetrapentylammonium (200 µM) applied from the equivalent of the outside, thus confirming orientation of these channels.

Supplementary Figure S2 (related to **Figure 5**)**. Custom-made MATLAB analysis for isolation of activity based on single channel properties.** This example illustrates analysis of five data segments representing various combinations of channel openings from a bilayer with two TREK-$2^{in/out}$ and two TREK-$2^{out/out}$ channels. (**A**) Red dots on top of the trace indicate *slope evaluation* points (see B and C), Data segments (black) are overlaid on colored lines that represent amplitude thresholds used to assign conductance (see panel D for color key). Each cluster is evaluated based upon a number of parameters (e.g. *slope* (see B and C), *closing frequency* and *immediate neighbor*. (**B**) Two simultaneously opened TREK-$2^{out/out}$ (left) have a conductance similar to a single TREK-$2^{in/out}$ (right), but different opening kinetics. (**C**) The slope evaluation points distinguish TREK-$2^{in/out}$ from TREK-$2^{out/out}$, and are given for each data point as the amplitude difference between the preceding point and that prior to the subsequent point. Examples of data slope points are shown in red dots above the traces; the cut-off threshold is set at 8 pA. (**D**) To distinguish "2x TREK-$2^{out/out}$ + 1 TREK-$2^{in/out}$" from "2 TREK-$2^{in/out}$", both the *slope value* and the *immediate neighbor* are considered because a single channel opening or closing is more likely than two channels opening and/or closing simultaneously.

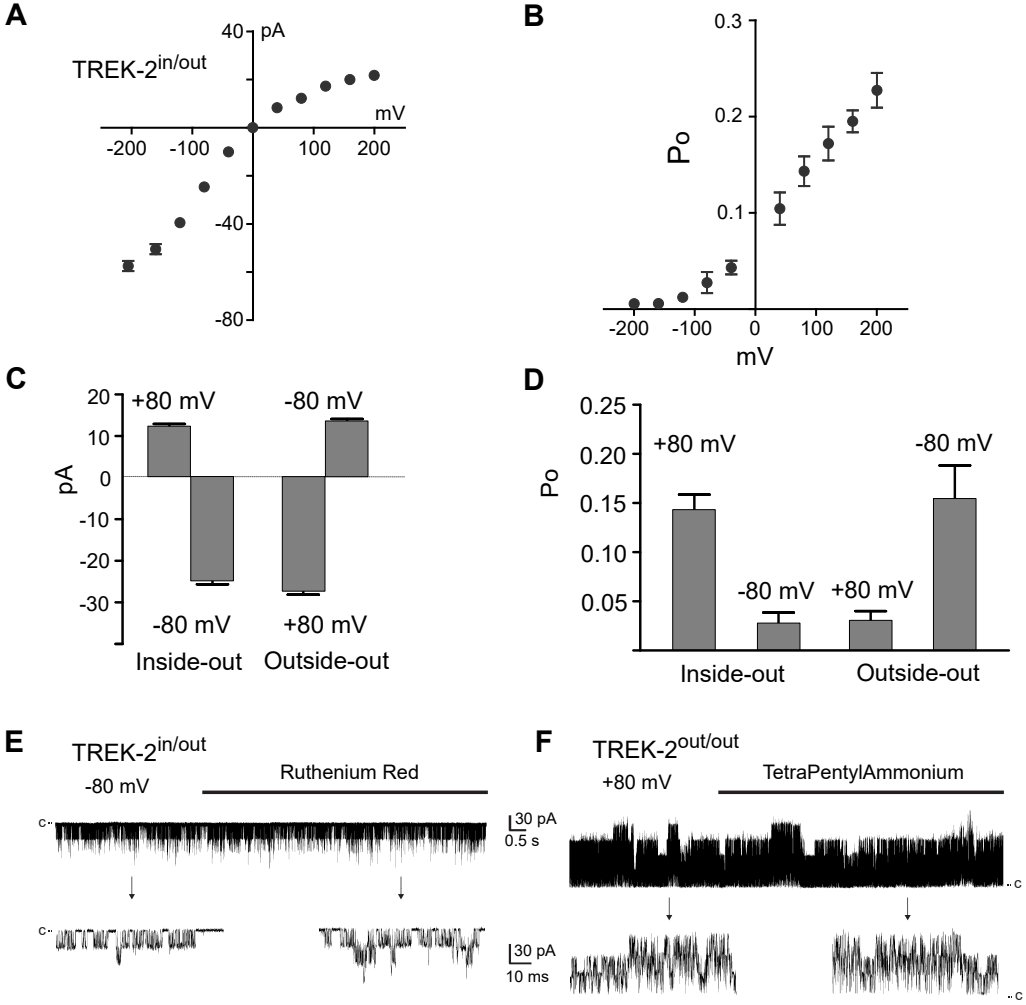
A
TREK-2in/out
40 pA
mV
-200 -100 100 200
-40
-80
B
Po
0.3
0.2
0.1
-200 -100 0 100 200
mV
C
pA
20 10 0 -10 -20 -30
+80 mV
-80 mV
-80 mV
+80 mV
Inside-out
Outside-out
D
Po
0.25 0.20 0.15 0.10 0.05
+80 mV
-80 mV
-80 mV
+80 mV
Inside-out
Outside-out
E
TREK-2in/out
-80 mV
Ruthenium Red
C
C
F
TREK-2out/out
+80 mV
TetraPentylAmmonium
30 pA
0.5 s
C
30 pA
10 ms
C

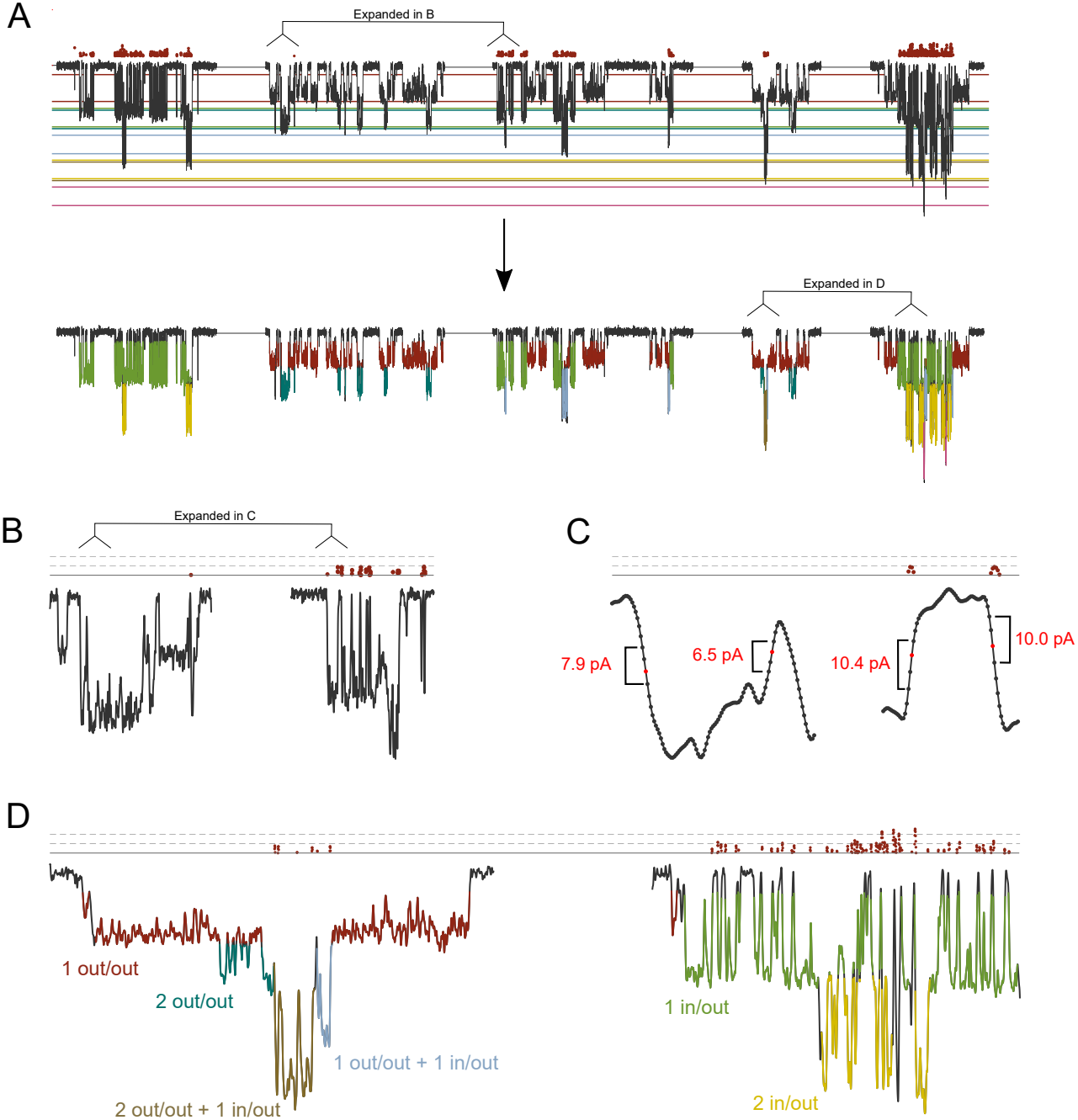
A
Expanded in B
Expanded in D
B
Expanded in C
C
7.9 pA
6.5 pA
10.4 pA
10.0 pA
D
1 out/out
2 out/out
1 out/out + 1 in/out
2 out/out + 1 in/out
1 in/out
2 in/out